Ottawa, Canada
INTER-NOISE 2009
2009 August 23–26

Loss factor estimation using the impulse response decay method on a stiffened structure

Randolph Cabell*
Noah Schiller
Structural Acoustics Branch
NASA Langley Research Center
Hampton, VA 23681 USA

Albert Allen
Mark Moeller
Spirit AeroSystems, Inc.
Wichita, KS 67278 USA

ABSTRACT

High-frequency vibroacoustic modeling is typically performed using energy-based techniques such as Statistical Energy Analysis (SEA). Energy models require an estimate of the internal damping loss factor. Unfortunately, the loss factor is difficult to estimate analytically, and experimental methods such as the power injection method can require extensive measurements over the structure of interest. This paper discusses the implications of estimating damping loss factors using the impulse response decay method (IRDM) from a limited set of response measurements. An automated procedure for implementing IRDM is described and then evaluated using data from a finite element model of a stiffened, curved panel. Estimated loss factors are compared with loss factors computed using a power injection method and a manual curve fit. The paper discusses the sensitivity of the IRDM loss factor estimates to damping of connected subsystems and the number and location of points in the measurement ensemble.

1. INTRODUCTION

High frequency energy models of vibrating structures require estimates of damping loss factors of subsystems or components of the structure. Due to the complex nature of damping, experimental methods are often the tool of choice for determining these loss factors, especially on novel structures or materials. Numerous references can be found on damping loss factor determination from experimental data (see, for example[1–7]). Methods for computing loss factors are based on either a modal, decay-rate, or power injection approach.[5] Modal approaches are suitable for well-spaced resonances, but become impractical at high modal density. Power injection methods require estimation of energy levels of connected components and knowledge of the mass of the structure. Decay rate methods require fewer measurements, but yield estimates of total loss factors, which include all forms of energy loss such as internal damping and energy transfer through boundaries to surrounding structural components, fluids, or supporting test fixtures.

The goal of the current paper is to examine an automated decay rate method applied to data from a limited portion of a complex structure. The envisioned application is one where the test engineer has access to only a portion of a structure for response measurements, thus rendering the power injection method impractical. A finite element model of an aircraft sidewall was chosen

*randolph.h.cabell@nasa.gov; noah.h.schiller@nasa.gov; albert.allen@spiritaero.com; mark.moeller@spiritaero.com

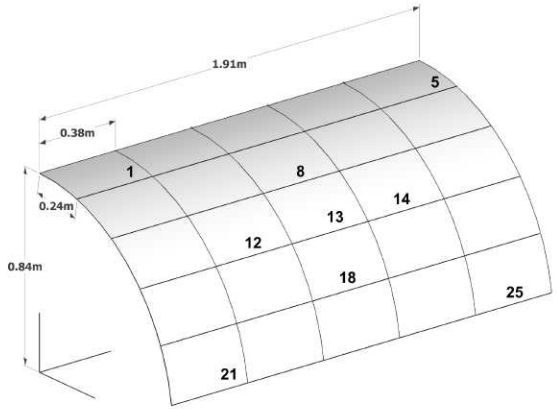


Figure 1: Dimensions and stiffener locations.

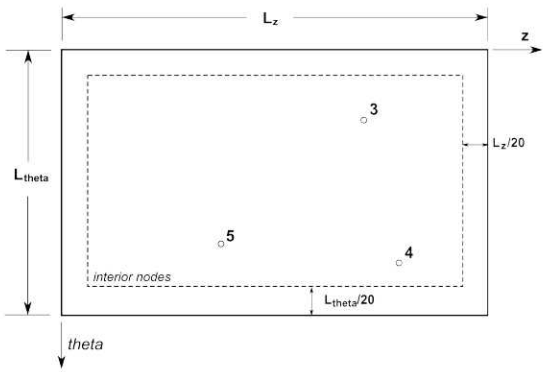


Figure 2: Drive point locations on panel 13.

for the study due to its mixture of global and local behavior depending on the frequency range of analysis. Trends in the computed loss factor versus frequency are related to loss factors computed from power injection methods and to the known loss factors of the components of the structure from the finite element model. The effect of an energy discontinuity between drive and response points on the computed loss factor is discussed.

The paper begins with a description of the numerical model of a curved, stiffened sidewall used to generate frequency responses. An automated procedure for computing loss factors from these frequency responses is then described. Results of applying the automated procedure to frequency responses for various combinations of component damping in the numerical model are then discussed, followed by conclusions.

2. ANALYSIS

The decay rate method discussed here assumes impulse responses are computed from band-limited frequency responses, and in turn normalized Schroeder decay curves are computed from the impulse responses.[9] A normalized Schroeder decay function at sampling instants t_k is computed from L samples of an impulse response, $h(t_k)$, as[7,9]

$$d(t_k) = \frac{\sum_{s=t_k}^{L} h^2(s)}{\sum_{s=0}^{L} h^2(s)} = 1 - \frac{\sum_{s=0}^{t_k} h^2(s)}{\sum_{s=0}^{L} h^2(s)} \tag{1}$$

Schroeder showed that the decay computed from a single impulse response is equivalent to an ensemble average of squared decays,[9] and hence is much smoother than Hilbert transforms of individual squared impulse responses.

A. Numerical Model

Frequency responses for this analysis were generated using a finite element model of a periodically stiffened, curved aluminum structure driven by a point force normal to the surface. The modeled structure is shown in figure 1. Curved, rectangular ring-frames were spaced at 0.38 m intervals along the z-axis, and rectangular stringers were spaced at 0.24 m intervals along the θ-axis; mid-planes of both stiffeners coincided with the mid-plane of the skin. Material properties and stiffener

Table 1: Properties and dimensions.

E	$7.0e10$ N/m^2
ν	0.33
ρ	2700 kg/m^3
skin thickness	0.001 m
ring frame width	0.01905 m
ring frame height	0.0508 m
stringer width	0.0508 m
stringer height	0.0155 m

Table 2: Node spacing.

1/3-octave center frequency (Hz)	spacing (mm)
$f <= 250$	16
$250 < f <= 500$	11
$500 < f <= 1250$	9
$1250 < f <= 2500$	8

Table 3: Damping variations for computational runs.

Computational run #s	Input location (see fig. 2)	Component loss factors
3,4,5	3,4,5	$\eta_{\text{skin}} = 0.015, \eta_{\text{stiffeners}} = 0.05$
13,14,15	3,4,5	$\eta_{\text{skin}} = 0.015, \eta_{\text{stiffeners}} = 0.05, \eta_{\text{drivenpanel}} = 0.05$

dimensions are given in table 1. The skin was modeled using CQUAD4 plate elements and the stiffeners were modeled using CBEAM elements. The nodal spacing was varied with analysis frequency, as listed in table 2, to ensure sufficient elements per structural wavelength without excessive grid sizes at low frequency. The panel edges in the z and θ directions were constrained to zero in-plane displacement.

A direct frequency response analysis in MSC Nastran™was used to determine the frequency responses. Damping in the direct frequency response is implemented as a complex stiffness.[10] The finite element analysis is inherently narrowband, hence decay curves for 1/3-octave bands were obtained by applying a bandpass, frequency-domain filter to frequency responses computed over a bandwidth slightly wider than each 1/3-octave band. To reduce the computational burden, the spacing between analysis frequencies varied depending on the 1/3-octave band. Since $\Delta f = T$, where T is the impulse response length, a criterion of $T_{60}/T = 0.3$ was used to determine T, where T_{60} is the time for an impulse response with a loss factor of 0.015 to decay by 60 dB. The loss factor of 0.015 corresponded to the minimum loss factor in the model. This approach easily satisfies the criterion suggested by Jacobsen[3] that $T_{60}/T < 2.5$.

Multiple computational 'runs' were performed for various locations of the normal input force and panel damping, listed in table 3. The locations of the force on the driven panel are indicated in figure 2. A single force was applied in each run, so for example, run 3 had a single force at location 3, while run 4 had a single force at location 4. The dashed rectangle in figure 2 labeled *interior nodes* denotes nodes spaced a small distance away from the stiffeners. Note that the only difference between runs 13–15 and runs 3–5 is an increase in damping of the driven panel from 0.015 to 0.05.

B. Automated IRDM procedure

An automated procedure was used to estimate decay rates of Schroeder decay curves. A linear regression[11] was used to determine the parameters of a simple exponential model of the decays, given by

$$\hat{d}(t) = c_1 e^{-c_2 t} \tag{2}$$

where $\hat{d}$ denotes an approximation of the measured decay, $d(t)$. This model is admittedly simple given the complexity and time-varying behavior of energy decay in coupled systems.[12] Nonetheless, application of this simple model is easily automated, and its use here is restricted to initial portions of energy decays.[3,6] The loss factor is given by $\eta = c_2/2\pi f$, where f is the center frequency of the band under study. The multiple correlation coefficient, R^2, was computed for each regression to quantify the correlation between $d(t)$ and $\hat{d}(t)$, where $0 \leq R^2 \leq 1$. A perfect fit, when $R^2 = 1$, indicates the data is perfectly described by equation 2. A less than perfect fit is caused by several factors, including measurement noise, time delay between the input and response points, beating between closely spaced resonances, decay rates of connected subsystems, and dynamics of bandpass filters applied to the data.[3,6,7]

Because most decay curves are more complicated than the simple exponential in equation 2, the results of the curve-fit will depend on the fitted portion of the decay curve.[3,6] Early decays are associated with total loss factors (combinations of damping and coupling), while later decays are more susceptible to measurement noise and filtering effects. In the current work, an exponential was fitted to the first [-2,-17] dB of decay, as suggested in the references.[3,6] In addition, a screening procedure was used to eliminate decays that deviated significantly from a simple exponential. While deviation from a simple exponential can be important, the screening was used here to eliminate impulse responses from bands with no resonances, which is primarily a low-frequency phenomenon. If $R^2 < 0.92$ or $\eta > 0.8$, the frequency response was removed from further analysis. These values were determined by examination of typical decay curves, and by consideration of the decay of the impulse response of the frequency domain window applied to the frequency responses.[3]

Once a set of frequency responses had been screened, the corresponding normalized Schroeder decays were averaged together, with no time-shifting, to obtain a single decay that was then fitted using equation 2. This averaging was done to reduce the variance of the estimated loss factor.

C. Manual IRDM procedure

Loss factors computed with the automated IRDM routine were compared with loss factors obtained by a manual procedure. A manual curve fitting procedure can be useful for dealing with non-ideal decays created by multiple slopes or high noise levels. It can be difficult to create an automated procedure that is robust to the variability seen in these types of decays. The manual procedure was applied to averaged Schroeder decay curves, similar to the automated procedure. The manual procedure fitted the earliest portion of the decay curve, where both the start and length of the fitted decay were left up to the judgment of the practitioner.

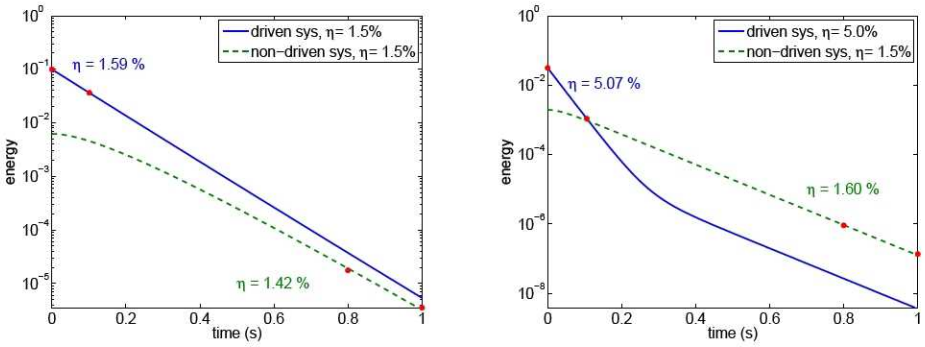
D. Transient SEA

Limitations of the exponential model in equation 2 are illustrated using a simplified transient SEA[13] model of two coupled subsystems. Assuming the damping of the ith subsystem is η_i and the coupling from i to j is η_{ij}, the rate of change of subsystem energies after input power is removed can be written[14]

$$\left[\frac{d\mathbf{E}(t)}{dt}\right] = -\omega \begin{bmatrix} \eta_1 + \eta_{12} & -\eta_{21} \\ -\eta_{12} & \eta_2 + \eta_{21} \end{bmatrix} [\mathbf{E}(t)] \tag{3}$$

The free responses of the two subsystems are given by the sum of exponentials

$$E_1(t) = A_1 e^{\sigma_1 t} + B_1 e^{\sigma_2 t}, \quad E_2(t) = A_2 e^{\sigma_1 t} + B_2 e^{\sigma_2 t} \tag{4}$$



(a) same damping in both subsystems. (b) higher damping in driven subsystem.

Figure 3: Energy decays in 2-subsystem model

where the A and B coefficients are determined by initial conditions. The exponents are given by the eigenvalues of the η matrix, which are entirely real, indicating the energy decays with no oscillation.[15] Even for this simple system, the rate of energy decay in either subsystem depends on relative values of damping and coupling in the two subsystems, and on initial conditions.[12]

Example decays for two coupled subsystems with equal modal density and are shown in figure 3. The coupling loss factor was 0.001. The initial conditions corresponded to a steady unit power applied to the driven subsystem, which was then set to zero at $t = 0$. Rates of decay, determined by a curve fit, are shown for the early decay of the driven system and later decay of the non-driven system. In both figures, the driven system's initial decay rate exceeds its damping loss factor due to energy sharing with the non-driven system. In figure 3(b), where the driven system's damping exceeds the non-driven system's, a dual-slope decay is evident. The decay rate of the non-driven system asymptotically approaches a value, subject to the initial condition, $dE_2/dt = 0$. In either case, the decay rate computed from a curve fit to either subsystem clearly depends on the portion of fitted decay. A fit that encompasses a transition between two slopes, such as at $t = 0.3$ sec in figure 3(b), will produce an intermediate decay rate.

E. Power injection method

Lyon postulated using the balance between transported and dissipated energy as a means of measuring damping.[13] This technique has become known as the Power Injection Method (PIM) for damping estimation. The loss factor is defined as the ratio of the energy lost per radian to the maximum potential energy of the system,[4,16] recognizing that at resonance, the maximum potential energy, or maximum strain energy, equals the maximum kinetic energy, or total energy, of the system. Off resonance, total energy is more difficult to define,[17] but either peak strain or peak kinetic energy were used here. Assuming a harmonic force input at frequency ω has complex amplitude F, and the structure has a complex velocity response v, the loss factor is given by

$$\eta = \frac{\mathrm{Re}\{Fv^{\star}\}}{2\omega E_{SE,peak}} \tag{5}$$

A global loss factor is obtained if $E_{SE,peak}$ corresponds to the peak strain energy of the entire structure. A local total loss factor, which includes damping losses and coupling losses, is obtained if $E_{SE,peak}$ corresponds to the peak strain energy of a smaller portion of the structure, such as a driven panel.

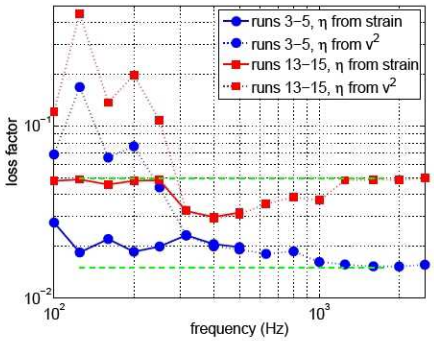


Figure 4: System loss factors from global PIM.

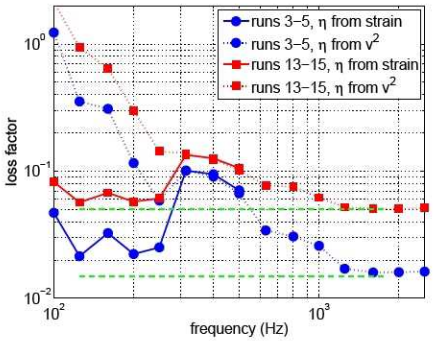


Figure 5: Loss factors from local PIM.

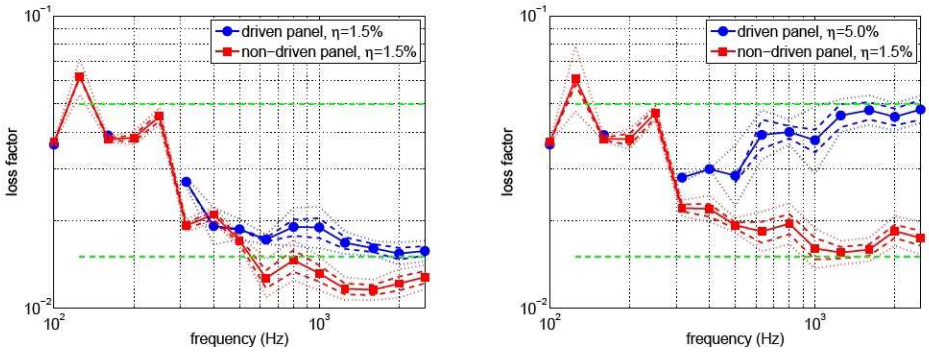
3. RESULTS

A. Loss factors from PIM

Loss factors were computed using the power injection method and either peak strain or peak kinetic energy from the finite element analysis. System loss factors, where the total energy of the structure was used in the denominator of equation 5, are shown in figure 4. The blue curves show loss factors averaged over runs 3–5 while the red curves show loss factors averaged over runs 13–15 (where the damping of the driven panel was increased to 5%). Solid lines, in both colors, indicate loss factors computed using peak strain energy, while dotted lines indicate loss factors computed using kinetic energy (elemental strains were computed only up to 500 Hz). The green dashed lines indicate the panel and stiffener loss factors of 1.5% and 5%.

For both sets of computational runs, the solid and dotted lines overlap above about 315 Hz, indicating a sufficiently resonant response to assume equality of peak strain and peak kinetic energy. The modal density drops below 315 Hz; there were 22 modes in band at 315 Hz, 8 modes at 250 Hz, and 2 modes at 200 Hz. Between resonances, the total energy is difficult to define in terms of either strain or kinetic energy.[17] However, because the band-averaged kinetic energy drops below the average strain energy, loss factors from kinetic energy greatly exceed those from strain energy below 315 Hz. Above 1000 Hz, the loss factors for both damping configurations approach the loss factor of the driven panel. Between 315 and 1000 Hz, the loss factor depends on the damping and fractional energy levels of the structure's components, and thus varies between the 1.5% panel damping and 5% stiffener damping.

Loss factors computed using a local PIM analysis are shown in figure 5. This local PIM was implemented using strain and kinetic energy of only the driven panel in the denominator of equation 5. This is equivalent to assuming all energy in the structure is dissipated within the driven panel. As expected, these local loss factors exceeded the system loss factors shown in the previous figure, especially at low frequencies where the response is more global than local. Nonetheless, the local loss factors approached the loss factor of the driven system above 1000 Hz. The sudden increase in loss factor from 250 to 315 Hz is a result of the increased modal density at 315 Hz. A narrowband analysis revealed that loss factors from strain energy were small between resonances and increased sharply at resonance. Conversely, loss factors from kinetic energy were high between resonances with sharp dips at resonances. As a result, the band-averaged loss factors computed from strain energy were much lower than those computed from kinetic energy.



(a) runs 3–5 (driven panel $\eta = 1.5\%$). (b) runs 13–15 (driven panel $\eta = 5\%$).

Figure 6: Loss factors from automated IRDM for two damping configurations.

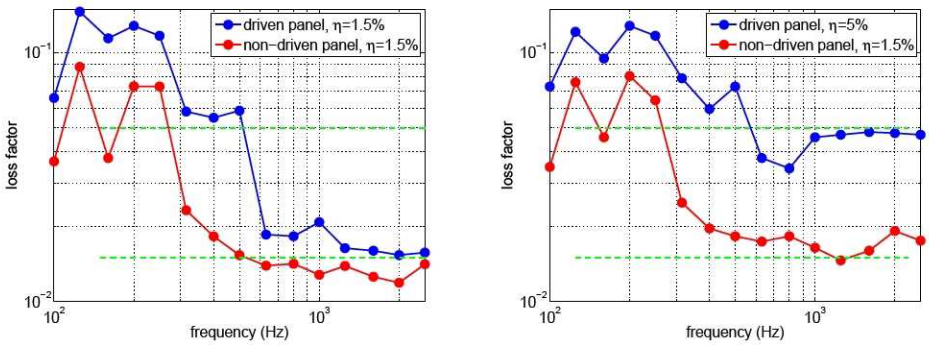
B. Automated IRDM results

Automated IRDM was applied to data from the same two damping configurations just discussed: computational runs 3–5 and 13–15. For each run, the effect of response point location was investigated for response points within the driven panel (panel 13), and response points outside the driven panel (panels 8, 12, 14, and 18). In both cases, response points were taken from an area a small distance away from the stiffeners (see figure 2). At each response point and 1/3 octave band, the frequency responses from the narrowband Nastran analysis were windowed using the magnitude of a 6th order Butterworth bandpass filter with corner frequencies at the boundaries of the 1/3 octave band. The impulse response was then computed via inverse FFT and the Schroeder decay computed. The initial -2 dB to -17 dB of each decay was fitted with the exponential in equation 2, followed by application of the screening procedure. Frequency responses with R^2 less than 0.92 or loss factors greater than 0.08 were removed from further analysis. The maximum acceptable loss factor was approximately equal to the loss factor of the frequency domain Butterworth window.

In order to study the probability distributions of estimated loss factors, response points were divided into sets of either 5 or 20. These set sizes were chosen arbitrarily to correspond to sparse and dense measurement arrays that might be used in an experimental study of loss factors. For each set of 5 or 20 points, the corresponding Schroeder decays from each of the three drive points were averaged together and a single loss factor obtained for that averaged decay curve. Thus each loss factor estimate consisted of an average of either 15 or 60 Schroeder decays. A log-normal distribution was assumed for the data, and means and variances computed for the estimated loss factors.

Figure 6 shows loss factors for the two damping configurations studied here. In the plots, the solid line indicates the mean loss factor at the 1/3 octave band center frequencies, while the dashed and dotted lines show two standard deviations about that mean for the 20-point and 5-point averages, respectively. The blue data correspond to response points in the driven panel; the red data correspond to response points outside the driven panel. The green lines are plotted at loss factors of 1.5% and 5%, for reference. It should be noted that many response points on the driven panel were within the direct field of the input force at low frequency. Application of the screening procedure eliminated nearly all of those points from the analysis, which explains the lack of data points on the blue curve below 315 Hz.

In general, estimated loss factors derived from response points in the driven panel approach



(a) runs 3–5 (driven panel $\eta = 1.5\%$). (b) runs 13–15 (driven panel $\eta = 5\%$).

Figure 7: Loss factors from manual IRDM for two damping configurations.

the loss factors of the driven panel above 1000 Hz. Loss factors derived from response points outside the driven panel underpredict the driven-panel loss factor above 1000 Hz. This agrees with observations from the transient SEA analysis in figure 3 that fitting the initial decay for points in the driven panel will overpredict the loss factor while fitting the initial decay for points outside the driven panel will underpredict the loss factor. The blue curve in figure 6(b) doesn't exceed the driven panel loss factor above 1000 Hz, as might be expected from this discussion. This could be due to multiple slopes in the decay, in which case the fitted decay slope will be a combination of slopes. The multiple-slope case and how it affects an automated curve-fit is an area worthy of further study.

Comparing the local PIM results (in figure 5) with the automated IRDM results shows that even though the automated IRDM results are computed from a velocity variable, the low and middle frequency results appear to be more reasonable than those from local PIM. The IRDM appears to better reflect the dynamics of the structural response and is less sensitive to bias due to unmeasured energy in the structure.

C. Manual results

Results of manually fitting the slopes of the Schroeder decay curves for the two damping configurations are shown in figure 7. The high frequency trend of the manual IRDM is similar to automated IRDM for points inside and outside the driven panel. However, for frequencies below 500 Hz, loss factors from the manual fit are generally higher than the automated fit. This is likely due to the flexibility of the manual fit relative to the rigid nature of the automated procedure. The automated approach estimated the slope of the first -2 dB to -17 dB of decay. The manual approach estimated the slope of the initial decay, whether or not that decay occurred within a fixed decay range. Thus, if multiple slopes were present, the manual approach was more likely to estimate the initial slope, and based on the transient SEA results (figure 3(b)), this initial slope will be higher than a later slope.

4. CONCLUSIONS

Three methods for computing loss factors from frequency responses were compared using data from a finite element model of a stiffened, curved shell. A power injection method was compared with a manual decay rate and an automated decay rate method. For the automated decay rate

method, Schroeder decays were assumed to decay as a single exponential and a linear regression was used to determine the decay rates over the first -2 dB to -17 dB of decay. Loss factors estimated using either decay rate method depended on the location of response points relative to the force input. When located within the same structural component as the applied force, the estimated loss factor approached the component's true loss factor above 1000 Hz. When an energy discontinuity, such as a stiffener, separated the response and drive points, the resulting loss factor depended on loss factors of components on either side of the discontinuity. Results from the automated procedure compared favorably with the manual curve fit above 500 Hz, however, below 500 Hz the manual fit produced higher loss factor estimates. This may be due to the presence of multiple decay rates causing the Schroeder decay to deviate from a single exponential. Either decay rate method produced better loss factor estimates below 1000 Hz than a local power injection method that used only the kinetic energy of the driven panel.

REFERENCES

[1] D.A. Bies and S. Hamid. *In situ* determination of loss and coupling loss factors by the power injection method. *Journal of Sound and Vibration*, 70(2):187–204, 1980.

[2] K. De Langhe and P. Sas. Statistical analysis of the power injection method. *Journal of the Acoustical Society of America*, 100(1):294–303, 1996.

[3] F. Jacobsen and D. Bao. Acoustic decay measurements with a dual channel frequency analyzer. *Journal of Sound and Vibration*, 115(3):521–537, 1987.

[4] Brandon C. Bloss and Mohan D. Rao. Estimation of frequency-averaged loss factors by the power injection and the impulse response decay methods. *Journal of the Acoustical Society of America*, 117(1):240–249, January 2005.

[5] M. Carfagni and M. Pierini. Determining the loss factor by the power input method (PIM), part 1: Numerical investigation. *ASME Journal of Vibration and Acoustics*, 121:417–421, July 1999.

[6] L. Wu, A. Ågren, and U. Sundbäck. A study of the initial decay rate of two-dimensional vibrating structures in relation to estimates of loss factor. *Journal of Sound and Vibration*, 206(5):663–684, 1997.

[7] Ning Xiang. Evaluation of reverberation times using a nonlinear regression approach. *Journal of the Acoustical Society of America*, 98(4):2112–2121, 1995.

[8] Julius S. Bendat and Allan G. Piersol. *Random Data*. Wiley-Interscience, New York, second edition, 1986.

[9] M.R. Schroeder. New method of measuring reverberation time. *Journal of the Acoustical Society of America*, 37(3):409–412, 1965.

[10] MSC.Software Corporation, Santa Ana, CA. *MSC Nastran Version 68 Basic Dynamic Analysis User's Guide*, 2004.

[11] N.R. Draper and H. Smith. *Applied Regression Analysis*. John Wiley and Sons, 2nd edition, 1981.

[12] G. Maidanik. Some elements in statistical energy analysis. *Journal of Sound and Vibration*, 52(2):171–191, 1977.

[13] Richard H. Lyon and Richard G. DeJong. *Theory and Application of Statistical Energy Analysis*. Butterworth-Heinemann, second edition, 1995.

[14] H.B. Sun, J.C. Sun, and E.J. Richards. Prediction of total loss factors of structures part III: Effective loss factors in quasi-transient conditions. *Journal of Sound and Vibration*, 106(3):465–479, 1986.

[15] R.J. Pinnington and D. Lednik. Transient statistical energy analysis of an impulsively excited two oscillator system. *Journal of Sound and Vibration*, 189(2):249–264, 1996.

[16] Daniel J. Inman. *Engineering Vibration*. Prentice Hall, Upper Saddle River, New Jersey, 2001.

[17] Eric E. Ungar and Edward M. Kerwin, Jr. Loss factors of viscoelastic systems in terms of energy concepts. *Journal of the Acoustical Society of America*, 34(7):954–957, 1962.